Biophysical Journal
Article

Biophysical Society

The Affinity of Sterols for Different Phospholipid Classes and Its Impact on Lateral Segregation

Thomas K. M. Nyholm,[1,*] Shishir Jaikishan,[1] Oskar Engberg,[1] Victor Hautala,[1] and J. Peter Slotte[1]
[1]Biochemistry, Faculty of Science and Engineering, Abo Akademi University, Turku, Finland

ABSTRACT Cholesterol is an essential molecule in the membranes of mammalian cells. It is known to be distributed heterogeneously within the cells, between the bilayer leaflets, as well as between lateral domains within the bilayer. However, we do not know exactly how cholesterol is distributed and what forces drive this sorting process because it extremely difficult to study using currently available methods. To further elucidate this distribution, we measured how cholesterol partitions between different phospholipid (PL) environments using different methods based on cholesterol, TopFluor-cholesterol, and cholesta-5,7,9(11)-triene-3-β-ol. Based on the obtained relative partition coefficients, we made predictions regarding how cholesterol would be distributed between lateral domains and between the inner and outer leaflets of the plasma membrane. In addition, using a *trans*-parinaric acid fluorescence-based method, we tested how cholesterol could influence lateral segregation through its interaction with unsaturated PLs with different headgroups. The results showed that the lower the affinity of cholesterol was for the different unsaturated PLs, the more cholesterol stimulated lateral segregation in a ternary bilayer of unsaturated PL/*N*-palmitoyl-D-*erythro*-sphingomyelin and cholesterol. Overall, the results indicate that both the distribution of cholesterol between different lipid environments and the impact of cholesterol on lateral segregation can be predicted relatively accurately from determined relative partition coefficients.

INTRODUCTION

Cholesterol is unevenly distributed within mammalian cells, and the cholesterol content in different membrane compartments varies markedly. Further, cholesterol is also distributed unevenly in the bilayer membrane, both laterally and between the inner and outer leaflets of the bilayer (1–3).

It is still unclear how the distribution of cholesterol between leaflets, lateral domains, and bilayer compartments is controlled, but it can be assumed that it is at least partially controlled by the interactions between cholesterol and other membrane lipids and proteins. It has repeatedly been shown that cholesterol has a particularly strong preference for sphingomyelin (SM) (4–7), and results from studies on lipid homeostasis suggest that cholesterol and SM are colocalized in the plasma membrane (8). Hence, it seems possible that by measuring the strength of the interactions between cholesterol and different phospholipids (PLs), knowledge about how the sterol is distributed both within and between cellular membranes can be obtained.

Many studies have convincingly demonstrated that cholesterol (and other sterols) have an increased affinity for PLs with saturated acyl chains when compared to PLs with unsaturated acyl chains (9–11). However, other properties also clearly influence the interactions between cholesterol and PLs, as indicated by the observation that cholesterol interacts more strongly with SM than with phosphatidylcholine, even with a matching acyl-chain order in the bilayers (4). As published data suggest, it can be expected that the PL headgroups would also influence the magnitude of the affinity that cholesterol has for the lipids (6,8,11–14). Because the different PL classes are distributed unevenly between the inner and outer leaflets of the bilayer, the interactions between cholesterol and lipids with different headgroups may be an important factor in determining the interleaflet distribution of cholesterol. In addition, the lateral organization within the bilayers may be influenced by the interactions between cholesterol and different PLs (7).

A reliable way to determine the affinity of cholesterol (and other sterols) for different PL environments is to use an equilibrium partition method that measures the partitioning of sterols between different PL bilayers or between PL bilayers and methyl-β-cyclodextrin (mβCD) in the aqueous

Submitted July 5, 2018, and accepted for publication November 19, 2018.
*Correspondence: tnyholm@abo.fi
Editor: Tommy Nylander.
https://doi.org/10.1016/j.bpj.2018.11.3135

phase (14–16). Here, we have measured the affinity of cholesterol, cholesta-5,7,9(11)-triene-3-β-ol (CTL), and TopFluor (TF)-cholesterol for lipid bilayers with different PL compositions using such approaches. This allowed the comparison of the partitioning behavior of cholesterol to that of the fluorescent analogs. An advantage of using fluorescent probes to analyze the interactions between sterols and PLs is that they allow studies with very low bilayer sterol content, low enough to eliminate the formation of sterol-rich domains or effects of sterols on the bulk membrane properties. This makes the interpretation of the data more straightforward and allows the determination of the affinity of sterols for PLs at low sterol concentration.

One important property of cholesterol is its ability to induce fluid-fluid phase separation, as has been observed in model membranes (7,17). In cell membranes, actual phase separation may not occur at physiological temperatures, but there is evidence that cholesterol can also induce lateral heterogeneity in cell membranes (18). Recently, it has been further shown that cholesterol-dependent phase separation occurs at subphysiological temperatures in cell-derived giant unilamellar vesicles (19). Therefore, it is clear that cholesterol-induced lateral heterogeneity is important and that several cellular processes are likely to be influenced by it. To determine the degree to which cholesterol facilitates the lateral segregation of lipids and the formation of nanodomains through interactions with the different PLs, we used a time-resolved fluorescence-based approach that is sensitive to the appearance of gel or liquid-ordered (l_o)-like domains in the bilayers (7,20). This was done in ternary lipid mixtures with varying unsaturated PLs, *N*-palmitoyl-D-*erythro*-sphingomyelin (PSM), and cholesterol.

The results from the equilibrium partitioning experiments showed that cholesterol (as well as the two fluorescent sterol analogs) had different affinities for saturated and unsaturated PLs with different headgroups. Interestingly, all three sterols showed similar PL preferences, and the affinity of the sterols for the different PLs correlated with the degree to which cholesterol facilitated lateral segregation in the ternary bilayers, including the different PLs. The usefulness of relative partitioning coefficients as a tool for predicting cholesterol distribution within cells, between bilayer leaflets, and between lateral domains will be analyzed and discussed.

MATERIALS AND METHODS

Materials

1-Palmitoyl-2-oleoyl-*sn*-glycero-3-phosphocholine (POPC), *N*-oleoyl-D-*erythro*-sphingomyelin (OSM), 1-palmitoyl-2-oleoyl-*sn*-glycero-3-phosphoethanolamine (POPE), 1-palmitoyl-2-linoleoyl-*sn*-glycero-3-phosphoethanolamine (PLPE), 1-palmitoyl-2-oleoyl-sn-glycero-3-phospho-L-serine (POPS), 1-palmitoyl-2-oleoyl-sn-glycero-3-phospho-(1′-rac-glycerol) (POPG), 1,2-dipalmitoyl-*sn*-glycero-3-phosphocholine (DPPC), 1,2-dipalmitoyl-*sn*-glycero-3-phosphoethanolamine (DPPE), 1,2-dipalmitoyl-sn-glycero-3-phospho-L-serine DPPS), 1,2-dipalmitoyl-sn-glycero-3-phospho-(1′-rac-glycerol) (DPPG), egg SM, and TF-cholesterol were obtained from Avanti Polar Lipids (Alabaster, AL). *N*-palmitoyl-D-*erythro*-sphingomyelin (PSM) was purified from egg SM by reverse-phase high performance liquid chromatography (Supelco Discovery C18 column, dimensions 250 × 21.2 mm, 5 μm particle size; Supelco, Bellefonte, PA) using methanol as eluent. The purity and identity of PSM was verified by electrospray ionization mass spectrometry. 1-Palmitoyl-2- diphenylhexatriene-*sn*-glycero-3-phosphocholine (DPH-PC) was purchased from Molecular Probes (Eugene, OR), and mβCD from Sigma Chemicals (St. Louis, MO). Cholesta-5,7,9(11)-triene-3-β-ol (CTL) was prepared according to published procedures (21,22). *trans*-parinaric acid (tPA) was synthesized and purified according to published procedures (23). It was stored at −87°C and contained 0.5 mol% butylated hydroxytoluene to prevent oxidation. Stock solutions of DPH-PC, TF-cholesterol, tPA, and CTL were prepared in ethanol. Fluorophore concentrations were determined based on the molar extinction coefficients of CTL (11,250 cm^{-1} M^{-1}), DPH-PC (92,000 cm^{-1} M^{-1}), TF-cholesterol (90,000 cm^{-1} M^{-1}), and tPA (88,000 cm^{-1} M^{-1}). The concentration of PLs was determined according to (24), and cholesterol concentration was determined using a surface barostat (25). Solutions were stored in the dark at −20°C and warmed to ambient temperature before use. The water used for all experiments was purified by reverse osmosis, followed by passage through a Millipore UF Plus water-purification system (Millipore, Billerica, MA) to yield a product resistivity of 18.2 mΩcm. All vesicles were prepared in buffer (50 mM Tris, 140 mM NaCl (pH 7.4)).

Equilibrium distribution of CTL between mβCD and LUVs

CTL partitioning between large unilamellar vesicles (LUVs) and mβCD was measured as described in detail in the Supporting Materials and Methods.

Equilibrium distribution of cholesterol between donor and acceptor vesicles

The equilibrium partitioning of cholesterol between large unilamellar donor vesicles (donor LUVs) and large unilamellar acceptor vesicles (acceptor LUVs) was determined using an anisotropy-based assay, described in detail in the Supporting Materials and Methods.

Equilibrium distribution of TF-cholesterol between donor and acceptor vesicles

The distribution of TF-cholesterol between donor LUVs and acceptor LUVs was studied using a Förster resonance energy transfer (FRET) approach in which the FRET donor was DPH-PC and the FRET acceptor was TF-cholesterol, described in detail in the Supporting Materials and Methods.

Calculation of sterol distribution based on relative partitioning coefficients

To use the determined relative partitioning coefficient to estimate the distribution of cholesterol (and the other sterols) in different lipids systems, an average relative partitioning coefficient was calculated using the following equation:

$$K_{R,Average} = \frac{PL_1K_{R,1} + PL_2K_{R,2} + \cdots + PL_nK_{R,n}}{PL_1 + PL_2 + \cdots + PL_n}. \quad (1)$$

This is a weighted average value, where PL_n is the number of a particular lipid (given, e.g., as the mol%) and $K_{R,n}$ is the relative partitioning coefficient of this particular lipid. This average K_R is calculated for a particular lipid composition, such as the outer leaflet of the plasma membrane. Having calculated the average K_R for both environments of interest (e.g., the inner and outer leaflets), the distribution of the sterol between them can be calculated simply by dividing the two average K_R parameters by each other.

Determination of lipid segregation based on tPA fluorescence

To study how the lipid bilayers segregated into lateral domains (either liquid disordered (l_d) and l_o or l_d and gel), the fluorescence lifetimes of tPA in bilayers were measured as a function of PSM concentration at 23°C. For these experiments, multilamellar vesicles were prepared by hydrating dry lipid films with argon-saturated buffer at 60°C for 30 min. After this, the samples were cooled to room temperature. The final lipid concentration in the samples was 100 μM (containing 1 mol% tPA). The formation of gel or l_o domains was detected by measuring the average fluorescence lifetime of tPA in a series of samples in which the molar fraction of PSM was increased in the samples while the cholesterol fraction was kept constant (between 0 and 20 mol%). The formation of gel or l_o domains was determined as the concentration of PSM at which the average lifetime function changed direction (because of a dramatically longer longest lifetime component).

RESULTS

CTL partitioning between PL vesicles and mβCD

CTL has been shown to be a good fluorescent cholesterol analog (26), and we have previously developed a method for measuring the equilibrium partitioning of CTL between LUVs and mβCD (10). Here, this method was used to determine how CTL interacted with PLs with different polar headgroups. Hence, we measured CTL partitioning between mβCD and LUVs composed of POPC, OSM, POPE, POPS, or POPG at 37°C. The results of these measurements are shown in Fig. 1, and calculated Gibbs free energies are shown in Table S1. The data in the figure show that the addition of an increasing amount of mβCD to the vesicles resulted in a concomitant decrease in the fluorescence anisotropy of CTL in the lipid bilayers (Fig. S1), which then can be translated into the fraction of CTL in the bilayers (Fig. 1 *A*) and in complex with mβCD. By fitting the data presented in Fig. 1 *A* with Eq. S2, the molar fraction partitioning coefficients (K_X) describing the equilibrium partitioning of CTL between the vesicles and mβCD could be determined. All determined partitioning coefficients are shown in Fig. 1 *B*.

The lowest partitioning coefficient was observed for acceptor LUVs composed of POPE, but POPG and POPC LUVs gave rise to only slightly higher coefficients. Markedly higher partitioning coefficients were measured with OSM and POPS LUVs. Based on earlier work with cholesterol, it was expected that CTL would have a high affinity for OSM bilayers (27). The high affinity of the sterol for POPS is also in good agreement with previous

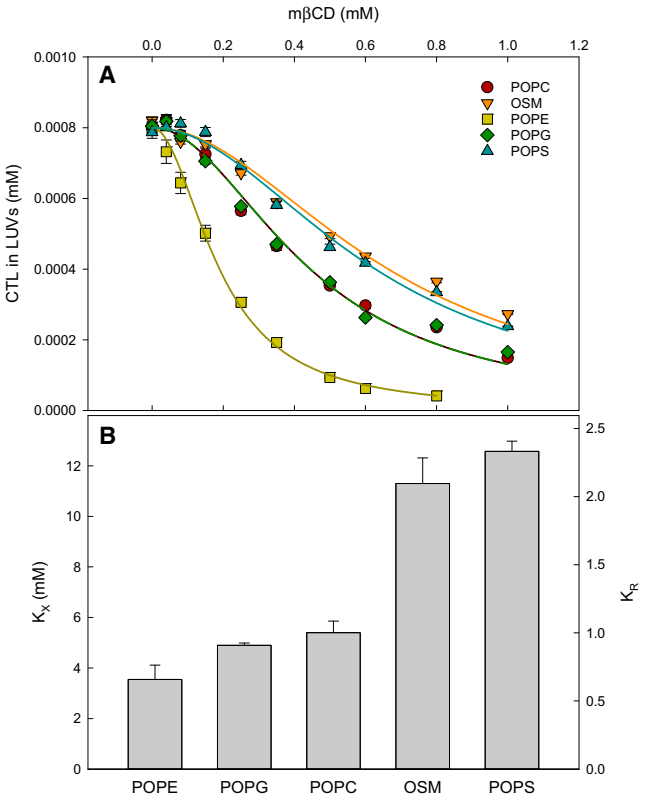

FIGURE 1 Equilibrium partitioning of CTL between LUVs and mβCD. (*A*) shows the amounts of CTL in the PL vesicles calculated from the anisotropy data shown in Fig. S1 using Eq. S1. The solid lines are the best fits that were obtained to the data with Eq. S2. (*B*) shows the molar fraction partitioning (K_X) and the relative partitioning (K_R) coefficients, which were determined at 37°C. Values are averages ± SD with $n \geq 3$. To see this figure in color, go online.

observations (11,14,28–30). However, that it would be as high as for OSM was not expected. This result is interesting because it suggests that monounsaturated phosphatidylserines in the inner leaflet could interact favorably with cholesterol and thereby influence both the lateral and *trans*-bilayer distribution of cholesterol in the bilayer.

TF-cholesterol partitioning between donor and acceptor LUVs

TF-cholesterol is a more recently developed cholesterol analog than CTL. Because of its fluorescence properties, it is more suitable for fluorescence microscopy than CTL. It has been shown to partition into an l_o phase (31). In FRET experiments, we observed that TF-cholesterol could not be removed from lipid bilayers with mβCD (Fig. S2). Apparently, the addition of the fluorescent group interferes with the formation of the cyclodextrin-cholesterol complex (32,33). Hence, partitioning of TF-cholesterol between mβCD and LUVs could not be studied. Instead, partitioning between donor and acceptor LUVs was measured.

To measure how TF-cholesterol was distributed between donor and acceptor LUVs, we used a FRET-based assay, in which the FRET between DPH-PC and TF-cholesterol was measured. Donor LUVs were prepared of POPC with 0.5 mol% DPH-PC and 0.5 mol% TF-cholesterol, as well as acceptor LUVs with varying compositions. Because the FRET efficiency depended linearly on the TF-cholesterol concentration in the donor LUVs (and DPH-PC remains in the donor LUVs), the data could be used to calculate the partitioning coefficient for how the sterol was distributed between the donor and acceptor LUVs (Figs. S3 and S4).

Similarly to CTL, the binding of TF-cholesterol to unsaturated PL bilayers with different headgroups was investigated. For this, POPC donor LUVs were mixed 1:1 with acceptor LUVs composed of pure POPC, OSM, POPE, POPS, or POPG and incubated overnight at 37°C to ensure that equilibrium had been reached (Fig. S5). Subsequently, the FRET efficiencies in the samples were determined by measuring the DPH-PC fluorescence lifetimes. From the FRET efficiencies, we calculated the relative partition coefficients (K_R, using Eqs. S4 and S5), which indicated the relative affinity of the sterol for the different PLs in relation to the POPC donor LUVs.

As is clear from the results shown in Fig. 2 (calculated Gibbs free energies are shown in Table S1), TF-cholesterol interacted differently with different PLs. The sterol seems to interact most strongly with POPS bilayers, closely followed by OSM. For POPE bilayers, the sterol showed a very low affinity compared to the other PLs, whereas the affinity for POPC and POPG was intermediate. These results resembled those obtained with CTL, suggesting that despite the structural differences between the two sterols, their relative affinity for the different PLs was similar.

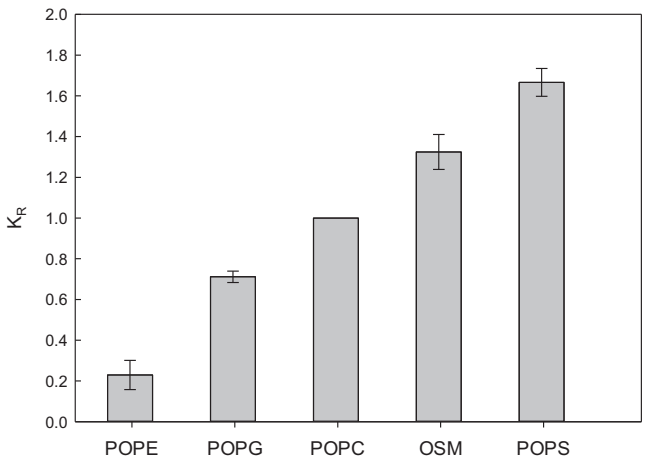

FIGURE 2 Relative partitioning of TF-cholesterol between different PL vesicles. The relative partitioning (K_R) between POPC and the other PLs was measured at 37°C using the FRET assay described in the methods section. Values are averages + SD with $n \geq 3$.

Cholesterol partitioning between donor and acceptor vesicles

To measure the partitioning of cholesterol between different PL bilayers, a setup based on donor and acceptor LUVs was chosen. In these experiments, the donor LUVs were composed of POPC with 25 mol% cholesterol and 1 mol % DPH-PC. The acceptor LUVs were composed of pure unsaturated PLs (POPC, OSM, POPE, POPS, and POPG). The donor and acceptor LUVs were mixed 1:1 and incubated overnight at 37°C, after which the fluorescence anisotropy of DPH-PC was measured at the same temperature. The measured anisotropies of DPH-PC indicated that the amount of cholesterol in the donor LUVs varied with the lipid composition in the acceptor LUVs (Fig. 3 *A*). To determine the amount of cholesterol in the donor LUVs, a standard curve for the DPH-PC in POPC bilayers with 0–35 mol% cholesterol was used (*inset* in Fig. 3 *A*). Using the standard

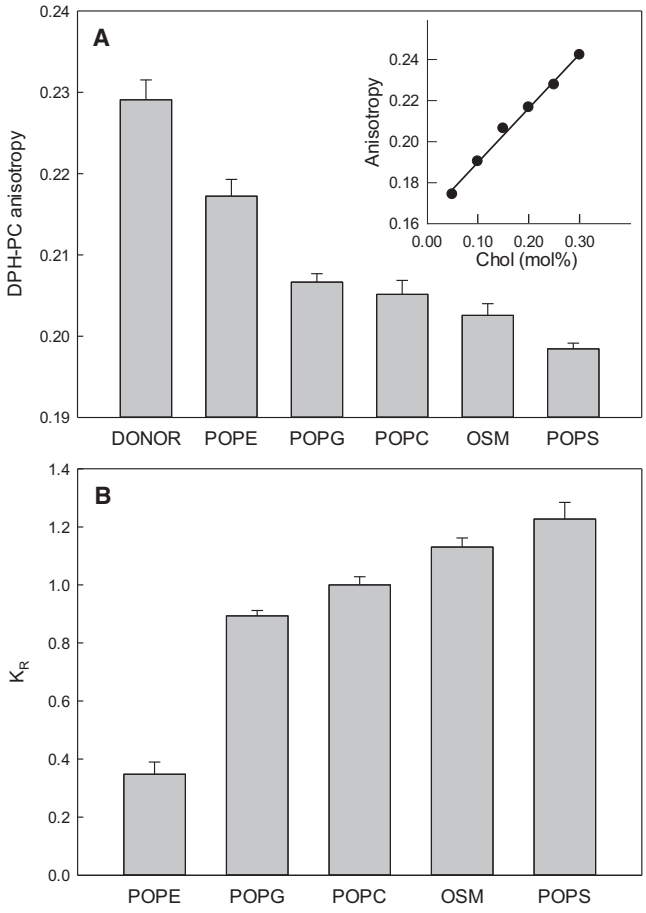

FIGURE 3 Equilibrium partitioning of cholesterol between different PL vesicles. The equilibrium partitioning of cholesterol between donor and acceptor LUVs was measured by monitoring the anisotropy of DPH-PC in the donor POPC LUVs initially containing 25 mol% cholesterol (*A*). The distribution of cholesterol between the LUVs was determined using a standard curve (*inset* in *A*). (*B*) shows the resulting relative partitioning coefficients (K_R) relative to POPC-POPC partitioning. Values are average + SD with $n \geq 3$.

curve, the amount of cholesterol in the acceptor and donor LUVs was calculated and the relative partitioning coefficient was determined (Fig. 3 *B*), and calculated Gibbs free energies are shown in Table S1. From the results, it is clear that cholesterol interacts most unfavorably with POPE, as can be seen from the low K_R. The other lipids interact more similarly with cholesterol, but the affinity of the sterol seems to be highest for OSM and POPS. Compared with the other two sterols, the cholesterol assay showed smaller differences in K_R between the different lipids (with the exception of POPE). We think this possibly could be due to the significantly higher sterol content in these experiments. With this much cholesterol in the bilayer, the bilayer as whole is affected by the sterol, whereas with less than ≤ 2 mol% sterol (as with CTL and TF-cholesterol methods), only local regions of the bulk bilayer are affected by the sterols. Indeed, it has been reported that the amount of cholesterol in the bilayer affects its partitioning behavior (15,34). However, even though the observed difference in the affinity of cholesterol for the different PLs was not as large as with the other sterols, the relative affinity of cholesterol for the PLs was again similar to data obtained with the fluorescence sterol analogs.

Sterol interactions with saturated PLs

As the interactions between PLs with saturated acyl chains and sterols are also of interest, we included such lipids in this study. First, the affinity of CTL for saturated PLs was investigated by measuring the equilibrium partitioning of CTL between mβCD and LUVs composed of 80% POPC and 20% DPPC, PSM, DPPE, DPPS, or DPPG at 37°C. With these compositions at this temperature, no gel phase formation occurred at the experimental temperature (data not shown), nor is it expected that l_o domains form (7,35). To have the same reference scale as in the experiments with the unsaturated lipids, a pure POPC sample was also included. The results from these experiments are summarized in Fig. 4 *A*, and calculated Gibbs free energies are shown in Table S1. The inclusion of all saturated lipids, except DPPE, led to increased membrane partitioning of CTL compared to pure POPC. This indicates that CTL favored all saturated PLs (except DPPE) over POPC. Overall, the results with the saturated lipids were similar to those with the pure unsaturated acceptor LUVs, with the exception that the affinity of CTL for LUVs containing DPPS was lower than for those containing DPPC or PSM, whereas the opposite was observed with unsaturated lipids. This indicates that the affinity of CTL for a PL bilayer is affected both by the acyl chains and the headgroup of the lipids and by the combination of these.

Similar experiments were also conducted with cholesterol (results in Fig. 4 *B*; Table S1). In these experiments, the interactions between cholesterol and saturated PLs were studied using acceptor LUVs consisting of 80 mol% POPC and 20 mol% saturated lipids (DPPC, PSM, DPPE, DPPS, or DPPG). As with the unsaturated lipids, the donor LUVs were composed of POPC with 25 mol% cholesterol and 1 mol% DPH-PC. Because of the high cholesterol/saturated PL ratio in these experiments, it is obvious that the results would show only very small differences between the different PLs (Fig. 4 *B*). Based on the results shown in Fig. 4, cholesterol partitioned similarly into the DPPG-, DPPS-, and DPPC-containing bilayers because the addition of these lipids to POPC did not seem to influence the affinity of cholesterol for the acceptor LUVs significantly. Meanwhile, the inclusion of PSM increased the affinity of the sterol for the donor vesicles, as seen from a small but significant increase in the partitioning coefficient. Gibbs free enegy for the transfer of cholesterol from POPC to POPC/PSM bilayers was calculated to be 0.35 kcal/mol; this is similar to what was observed in a previous study (34). The lowest preference for the acceptor LUVs was achieved with POPC/DPPE vesicles. This suggests that

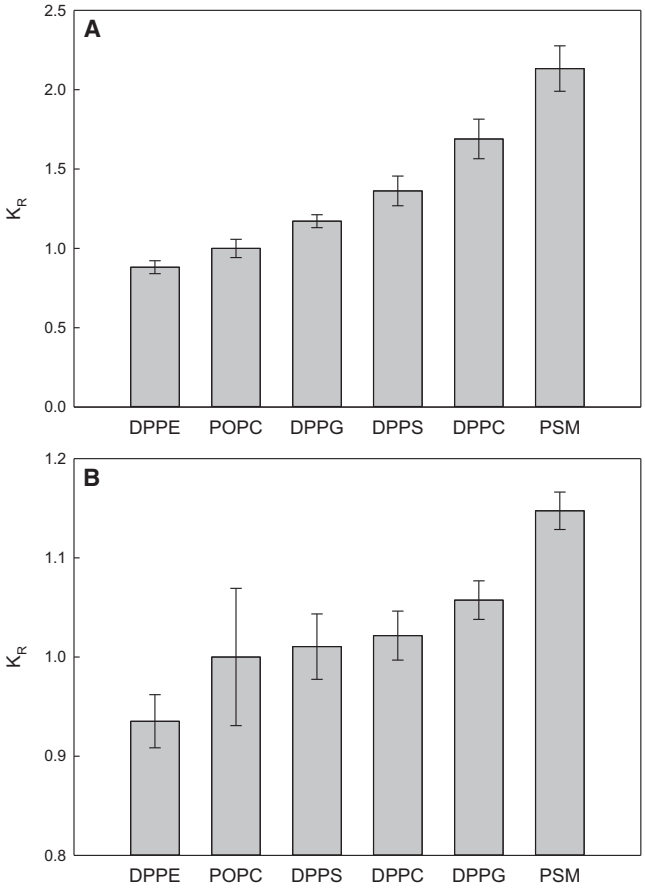

FIGURE 4 The preference of sterols for saturated PLs. CTL partitioning between LUVs composed of POPC/saturated PL (80:20) and mβCD was measured at 37°C. The resulting K_X are presented as K_R relative to pure POPC LUVs in (*A*). The relative partitioning of cholesterol between POPC donor LUVs and acceptor LUVs composed of POPC/saturated PL (80:20) at 37°C is shown in (*B*). Note the scale on the *y* axis in (*B*). Values are averages + SD with $n \geq 3$.

cholesterol interacts poorly with phosphatidylethanolamine (PE) molecules, likely because of the relatively small headgroup found in these molecules.

Lateral segregation in the lipid bilayers with and without cholesterol

It has previously been observed that the relative affinity of cholesterol for the different PLs in a bilayer correlates with both how prone the system is to form an l_o domain as well as with the properties of the formed l_o domains (7). Hence, it was of interest to test how the unsaturated lipids studied within this project could influence the transition from pure l_d bilayers to bilayers in which l_d and l_o domains coexist through their different interactions with cholesterol. By measuring the fluorescence lifetimes of tPA in lipid bilayers as a function of the molar fraction of PSM, the critical PSM concentration required for the formation of l_o domains could be determined. Fig. 5 *A* shows the results from measurements done with POPC bilayers having a constant cholesterol content (0, 10, 15, or 20 mol%) and an increasing PSM concentration (0–50 mol%) at 23°C with 1 mol% tPA. As can be seen in the figure, the average fluorescence lifetime of tPA increased with the PSM content, and at a critical mol% PSM, a more dramatic increase is observed, resulting in a clear change in slope. As a result, the data is better fitted with two linear functions, and the point at which these cross each other is the concentration of PSM at which

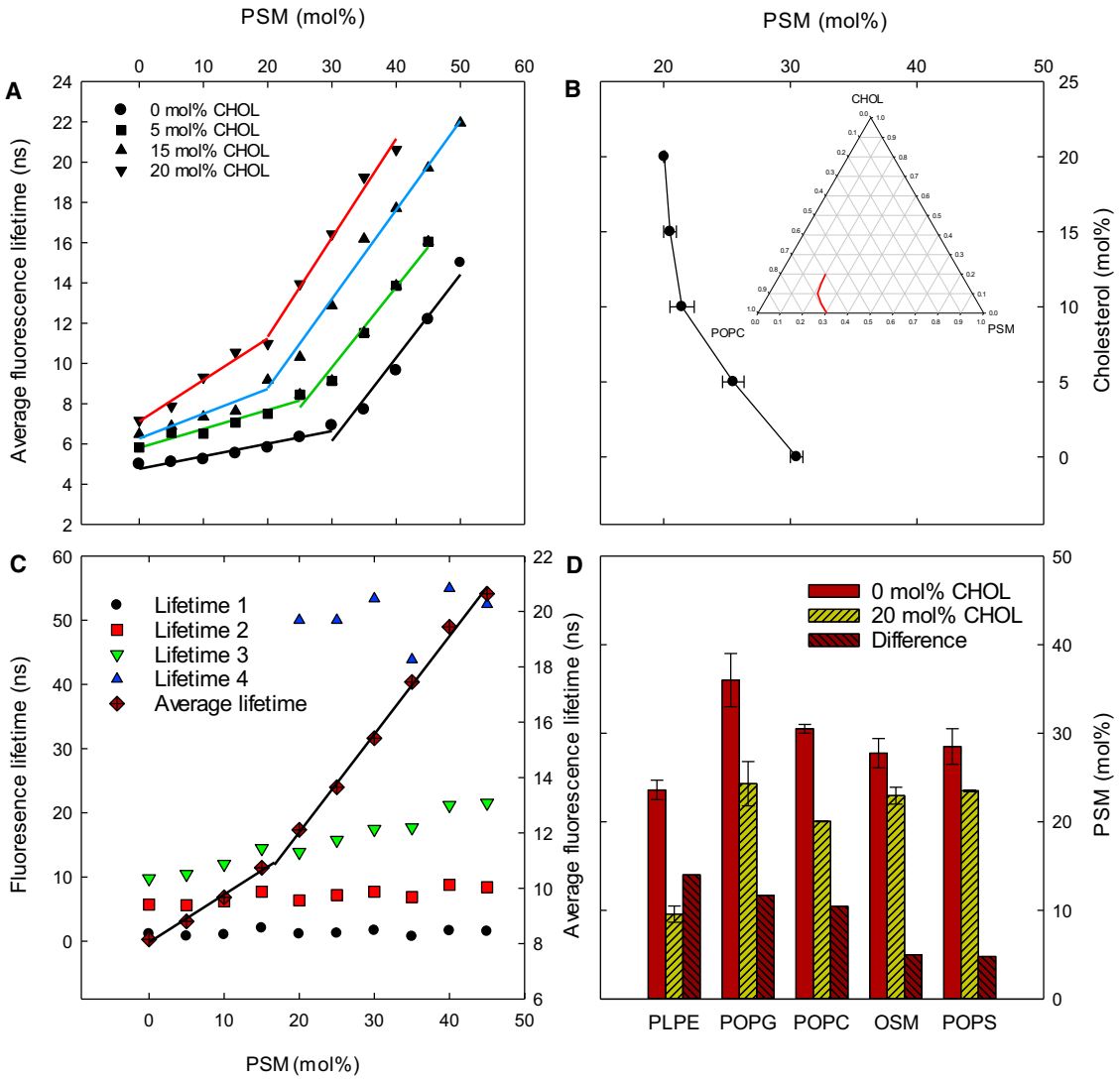

FIGURE 5 Influence of cholesterol and PL headgroup on the lateral segregation. (*A*) shows the tPA fluorescence lifetimes (representative data) as a function of PSM content at different cholesterol concentrations together with POPC at 23°C. The PSM concentration at which these trendlines change slope defines the PSM content at which the lateral segregation was initiated. For the POPC-based bilayers, these are summarized in (*B*) (values are averages + SD with $n \geq 3$.). (*C*) shows representative lifetime components observed in different ternary mixtures of PLPE, PSM, and 5 mol% cholesterol. The impact of different headgroups in the unsaturated lipids on the formation of the gel and l_o phases (and the difference between these two) by PSM at 23°C is quantified in (*D*). These values are averages + SD with $n \geq 3$. To see this figure in color, go online.

lateral domains with a higher degree of order (gel or l_o) start to form (20). In the series without cholesterol, gel domains start to form at ~30 mol% PSM, and the addition of cholesterol lowers the amount of PSM that is needed to form gel/l_o domains (quantified in Fig. 5 *B*). At ~10 mol% cholesterol, the boundary between l_d and the ordered phase (gel or l_o) changes direction. This change of direction is interpreted to be due to a change in the nature of the ordered phase (gel below and l_o above ~10 mol% cholesterol).

In Fig. 5 *C*, the individual lifetime components of a typical fluorescence decay of tPA are shown (PLPE/PSM/cholesterol with 5 mol% cholesterol). Commonly, three to four lifetime components were needed to achieve a good fit to the experimental data. As is clear from Fig. 5 *C*, a fourth lifetime component needed to be added to samples with ≥20 mol% PSM, that is, above the discontinuity in the lifetime function. Because this fourth lifetime component is longer than the other ones, it indicates that at this PSM concentration, a new, more ordered lipid environment was formed.

When the mol% PSM needed to form gel and l_o domains in bilayers containing different unsaturated PLs was compared, we observed that the headgroup structure affected both l_d-gel and l_d-l_o transitions (Fig. 5 *D*). Because the primary interest was to establish the impact of cholesterol on lateral segregation, the fraction of PSM needed to start the transition from the l_d to gel phases was compared with that needed to form l_o at 20 mol% cholesterol. The 20 mol% cholesterol trajectory was chosen because the largest shift of the boundary was observed with this cholesterol concentration in all PL samples studied. Because the experiments were performed at 23°C, we could not use POPE as a low-T_m lipid because of its l_d-gel transition at ~25°C. Instead, PLPE was used as the low-T_m phosphatidylethanolamine. With PLPE/PSM bilayers, we were not able to determine the transition from l_d to l_o at 20 mol% cholesterol. However, with up to 15 mol% cholesterol, the l_o boundary could be determined from the clear discontinuity in the lifetime function (Fig. S6). We assumed that this was the largest shift of the boundary (caused by cholesterol inclusion) because the boundary was at ~10 mol% PSM from 10 to 15 mol% cholesterol (Fig. S6). However, we also performed additional FRET experiments in which it was confirmed that l_o domains started to form above 10 mol% PSM in the PLPE/PSM/cholesterol bilayers (Fig. S7). Of the compared PLs, the largest effect of cholesterol inclusion was observed with PLPE-containing bilayers, in which lateral segregation occurred at ~15 mol% lower PSM concentration with cholesterol than without. In POPG- and POPC-based bilayers, the impact of cholesterol on lateral segregation was similar but smaller than observed with PLPE. In bilayers in which POPS and OSM were the low-T_m lipids, the effect of cholesterol was small, and the phase transition was lowered only ~5 mol% PSM when cholesterol was included.

When the observed effects of cholesterol on lateral segregation are compared to the affinity of sterols for the different unsaturated PLs, it is clear that the higher the affinity the sterol showed toward the lipid, the smaller the impact cholesterol had on lateral segregation in the bilayer.

DISCUSSION

The composition of the membranes in mammalian cells is complex, and it has proven extremely difficult to obtain detailed information about the arrangement of these components from direct studies of cells and their membranes. However, by studying how the different components interact and organize themselves in model membranes, we obtain data that help us predict the architecture of the cellular membranes and deepen our understanding of how they function. In this work, we measured the partitioning of sterols between bilayers and investigated how the observed PL interactions influenced lateral organization within the bilayer, finding a clear correlation between these events.

Sterol affinity for different PLs

Cholesterol is an essential component in mammalian membranes, and it is known to be involved in many cellular functions (2,36). Through its interactions with the other lipid components in the membranes, cholesterol can promote lipid segregation and the formation of lateral domains, often called lipid rafts (7,37–39). The intermolecular interactions between cholesterol and different PLs control this process, and by understanding these interactions we come closer to understanding the formation of lateral domains and the role they may play in cells.

Several different approaches have been used to study cholesterol partitioning between vesicles or vesicles and cyclodextrin (11,14,15,27,40). In this work, we used three different approaches, two of which use fluorescent analogs of cholesterol. A clear advantage of using a fluorescent sterol analog is that very low sterol concentrations can be used. This makes the interpretation of the data more straightforward because the bulk effects of sterols on the overall membrane properties and phase separation can be avoided. It also allows us to compare how the sterol partitions in lipid environments with lower sterol content, such as l_d phases. The results with the methods based on fluorescent analogs were also very similar to those using the cholesterol-based approach (Fig. S8). Using expensive lipids, it is also an advantage that very small amounts of lipids are needed for each assay.

When the interactions of the three sterols with the different unsaturated PLs were compared, it was clear that the relative affinities for the PLs was similar for all three sterols (POPE < POPG < POPC < OSM < POPS) (Figs. 1, 2, and 3; Table S1). These results were in agreement with previous observations (6,11,12,14), although published results

from DSC measurements have suggested that cholesterol interacted more strongly with SM than with PS (12). However, the magnitude of the difference in the affinity for different lipids depended on the sterol that was used (Fig. S8). Clearly, the smallest difference between the different PLs was observed with cholesterol. This may be partially due to the low sensitivity of the method, but more likely it was due to the higher sterol content used in these experiments. The lower concentration of sterol used with the fluorescent sterols (more than 10 times lower) eliminates the bulk ordering effect of the sterols on the lipids and should thus be more dependent on the intermolecular interactions. The effect of the high cholesterol concentration was even more evident in the experiments with POPC/saturated PL (80:20), in which only the bilayers containing PSM or DPPE clearly differed from the rest (Fig. 4). Significantly clearer differences between the different lipids were observed in the CTL partitioning experiments. Interestingly, with saturated lipids, cholesterol did not interact as favorably with PS as with the unsaturated lipids, which suggests that the combination of an acyl chain and headgroup can also determine how sterols interact with a PL. It is also noteworthy that the sterols had a lower affinity for DPPE than for POPC (Fig. 4), although DPPE seems to partition significantly into l_o domains, at least when fluorescent probes are linked to the headgroup (41,42).

Cholesterol is known to favor saturated over unsaturated acyl chains, and at least for CTL, the affinity for PL bilayers seem to correlate with the acyl-chain order (10,27). However, the high affinity is not due to acyl-chain order alone because other molecular features also influence the interactions between sterols and PLs (4). In this study, it was observed that both cholesterol and CTL preferred POPC over DPPE, and TF-cholesterol had about as high an affinity for POPS and OSM as has been reported for DPPC (7). These findings support the role of other molecular features besides acyl chains in the determination of the affinity of sterols for PLs.

Comparing how CTL, TF-cholesterol, and cholesterol partition between POPC and fluid PSM (Fig. S9), it is obvious that the sterol structure influences the degree to which a sterol prefers saturated over unsaturated chains. This, of course, was expected because it is well known that sterols with different structures interact differently with PLs (26,43–45). However, it is a good reminder that when using fluorescent analogs to gain insight into cholesterol distribution, for example, within cells, the analogs may behave differently than cholesterol. Still, both CTL and TF-cholesterol showed similar relative partition behavior as cholesterol, supporting their usefulness.

By obtaining the relative partitioning coefficient describing the distribution of cholesterol between different PL bilayers, we hoped to gain insight into how cholesterol is distributed within cells and how its presence can shape the membrane. One can ask how well relative partitioning describes the behavior of the sterol in complex bilayers. Compared with the way in which cholesterol partitions between the l_d and l_o domains calculated based on phase diagrams for ternary lipid mixtures, it is clear the partitioning between lateral domains is not the same as that between pure PL bilayers (5,46,47), although there are similarities. For instance, cholesterol partitions more into l_o domains the more *cis* double bonds there are in the unsaturated lipids. Further, cholesterol partitions more into the l_o domains when the saturated lipid is SM rather than PC, which is exactly what would be predicted based on our findings (7). In POPC/brain-SM/cholesterol bilayers, the K_R (l_o/l_d) for cholesterol is ~4, which is much lower than what has been reported for partitions between POPC and PSM bilayers (~12) (5,34). However, because SM is present in both the l_o and l_d phases, this should be taken into account in the calculations. When we correct for this and use the partition coefficients for bilayer-bilayer partition (using Eq. 1), we obtain an estimated K_R (l_o/l_d) of 2.85, which is closer to the K_R (l_o/l_d) obtained from the phase diagrams. Likely, other factors such as the cholesterol content in the two phases should still be taken into account to obtain a more accurate prediction. However, we think that it is clear that by measuring how cholesterol partitions between bilayers of different lipids, one can roughly estimate how cholesterol is distributed between lateral domains in membranes.

Lateral segregation

We have previously shown that the relative affinity of cholesterol for the unsaturated and saturated PLs in a ternary system affects the tendency of the system to segregate into lateral domains with different lipid compositions (7). From the cited study, it was clear that when the number of double bonds in the unsaturated PL was increased, the affinity of cholesterol for the lipid decreased and the tendency to form lateral domains increased in ternary lipid mixtures. Based on molecular dynamics simulations, it has been suggested that cholesterol drives the lateral segregation of unsaturated and saturated lipids because of enthalpy gain from more favorable van der Waals interactions between saturated acyl chains and cholesterol, and that unfavorable entropic contributions are working against the l_o domain formation (24). In this study, we observed that changes in sterol affinity, resulting from headgroup structure, also affected the membrane's tendency to segregate laterally in a similar way (Fig. 5). Commonly, the thermal stability of lateral domains is used as a measure of how prone a lipid mixture is to form domains (41,48–51). This parameter is mostly dependent on the lipid composition of the domains, and the higher the fraction of sterol and saturated PL is, the higher the melting temperature becomes. The approach we have used here is to determine the critical PSM concentration at which lateral domains appear at a constant temperature. This

indicates the solubility limit of PSM in the fluid phase at this temperature. Because we do not have phase diagrams describing the phase behavior of all the studied lipid mixtures, we chose to follow sample trajectories along a constant cholesterol concentration. The concentration 20 mol % was chosen because the available phase diagrams suggest that we should observe the formation of l_o domains and not gel domains at this cholesterol concentration, at least at low PSM concentrations (5,35,52,53). Because it is expected that the different unsaturated PLs will mix differently with PSM, we cannot determine the effect of cholesterol on lateral segregation in the different systems without understanding the cholesterol-free systems. Therefore, we used the same tPA-fluorescence-based approach to determine the PSM concentration at which PSM-rich gel phases start to form in binary bilayers composed of the different unsaturated lipids and increasing amounts of PSM. This PSM concentration is the highest fraction of PSM that is soluble in the l_d phase at this temperature. In all the studied systems, the addition of cholesterol lowered the solubility of PSM in the l_d phase in a concentration-dependent manner (Fig. 5, *A* and *B*), that is, cholesterol facilitated the formation of both gel (below ~10 mol% cholesterol) and l_o (above ~10 mol% cholesterol) domains. This effect of cholesterol may be expected because cholesterol, according to determined phase diagrams, does partition favorably into both gel and l_o phase as compared to the l_d phase (5,54). In fact, it would be surprising if cholesterol did not influence the formation of gel and l_o domains.

Comparison of the effect of cholesterol on the solubility of PSM in bilayers composed of the different unsaturated PLs showed that the solubility in PLPE was most affected by cholesterol, whereas the smallest influence was observed in the OSM and POPS bilayers (Fig. 5 *D*). The overall trend was that the influence of cholesterol on the PSM solubility in the l_d phase increased with decreasing cholesterol affinity for the unsaturated PL. These results agree with our previously published results, showing that the relative affinity of cholesterol for the two PLs in the bilayer determines how much PSM is needed to start the transition from the l_d to the l_o or gel phases (7). Therefore, one can argue that the results of both of these studies show that the lateral organization of lipids in bilayers is governed by both push and pull mechanisms (55).

The molecular shape of PE can likely explain the observation that cholesterol disliked PE both in partitioning and lateral domain formation experiments. The interactions between phospholipids and cholesterol have also been described in the umbrella model (56), which predicts that the small headgroup of PE makes the interactions between cholesterol and PE more unfavorable that those between, e.g., PC and cholesterol. In addition, it has been shown that cholesterol inclusion in PE bilayers facilitates the formation of the hexagonal phase (45). Hence, it may be expected that colocalization of PE and cholesterol in a bilayer would increase the intrinsic pressure in bilayers formed of these two lipids. Removal of some of the cholesterol from the PE bilayers into cyclodextrin complexes/acceptor LUVs or by lateral segregation of cholesterol and PE may therefore decrease the curvature stress in the bilayer. This suggests that lateral segregation, at least in this case, could be driven by the bilayer's tendency to strive for the least possible curvature stress. Phosphatidylcholines with multiple double bonds, especially those with double bonds in both acyl chains, can also have a molecular shape that introduces a curvature stress in the bilayers. Hence, the introduction of curvature stress could be the force behind the large impact of cholesterol on the lateral segregation in bilayers containing highly unsaturated PC molecules (7).

Biological implications

Cholesterol is unevenly distributed within the eukaryotic cell, and the concentration in the membranes increases along the secretory pathway, from the endoplasmic reticulum toward the plasma membrane, which is the membrane most enriched in cholesterol (1). It is believed that this cholesterol gradient plays an important role in the sorting of transmembrane proteins within the cell.

It has long been clear that PLs are distributed heterogeneously between the inner and outer leaflets of the plasma membrane (reviewed in (3)). However, the distribution of cholesterol between the two leaflets has remained unclear (3). In recent molecular dynamics simulations, it has been observed that cholesterol distributes evenly (although with a slight preference for the outer leaflet) in membranes designed to mimic cellular plasma membranes (57,58). Considering the relatively high content of cholesterol in the plasma membrane, these results seem reasonable. If we use the determined partition coefficients and lipid composition used in simulations, we can make a rough estimation of how cholesterol would partition between the two leaflets (disregarding the presence of the lipids for which we do not have a partitioning coefficient). We obtain an average distribution of 62% of the cholesterol in the outer and 38% in the inner leaflets of average cells, and in brain cells, the distribution would be 64 and 36%, respectively (calculated using Eq. 1; see Table S2 for details). In these calculations, we disregarded the presence of polyunsaturated acyl chains. If they were to be included in the calculation, the fraction of cholesterol in the outer leaflet would be even higher. In both cell types, we have a higher fraction of cholesterol in the outer leaflet than suggested by the computer simulations. One reason our calculations overestimate the amount of cholesterol in the outer leaflet could be that the fraction of cholesterol in the cell membranes is higher than that used in our experiments. As the cholesterol/PSM ratio increases, the impact of PSM on the distribution of cholesterol decreases. Similarly, we observed a much smaller impact of adding 20 mol% PSM to POPC bilayers when we measured

the partitioning of 25 mol% cholesterol than when we measured the partitioning of 2 mol% CTL (Fig. 4). With a high cholesterol content, an l_o phase may also be present, which we know has an impact on the partitioning behavior of sterols (20). Hence, a deeper understanding of cholesterol partitioning with varying cholesterol levels is needed before we can improve these predictions. Likely, many other parameters may also influence how cholesterol is distributed between the leaflets, i.e., the lipid packing density in the leaflets, etc. By gaining deeper insight into the interactions between cholesterol and phospholipids, we may eventually be able to perform calculations that are more exact.

The distribution of cholesterol between the inner and outer leaflets has been estimated using the fluorescent cholesterol analogs dehydroergosterol and CTL (59). It was reported that the majority of the fluorescent sterols were located in the inner leaflet (59). Here we estimated a larger fraction of CTL than of cholesterol in the inner leaflet (Table S2), and we observe differences in partitioning behavior between CLT and cholesterol that could explain the observations made with CTL in cells. For example, the relative affinity for PSM is markedly higher for cholesterol than for CTL, whereas the opposite was observed for the inner-leaflet lipid POPS. Particularly in membranes in which the cholesterol content is approaching 50 mol% of all lipids, the competition of CTL and cholesterol for interactions with the PLs may push CTL more to the inner leaflet while cholesterol may remain evenly distributed or even located foremost in the outer leaflet.

The role of the lipids of the inner leaflet in the formation of lateral domains in cell membranes has been addressed in several studies (60–62). We observed that both the high affinity of cholesterol for unsaturated PS and the low affinity of the sterol for unsaturated PE affected the formation of l_o domains (Figs. 4 and 5). It is plausible that the preferential interactions of cholesterol with PS over PE could be a driving force that shapes the lateral structure of the inner leaflet in combination with the unfavorable interactions between polyunsaturated acyl chains and cholesterol (63). Such cholesterol-dependent lateral segregation of two unsaturated PLs has been reported previously (7).

CONCLUSIONS

In this study, we determined the equilibrium partitioning of CTL, cholesterol, and TF-cholesterol between different PL bilayers and observed that the PL headgroup had a marked effect on the sterol affinity for the lipids. In experiments examining the effect of cholesterol on lateral segregation in bilayers composed of PSM, cholesterol, and different unsaturated PLs, we observed that the affinity of cholesterol for the unsaturated lipids correlated with the degree to which cholesterol facilitated the segregation. Based on analysis of the data, we can conclude that knowledge of how cholesterol partitions between different PL bilayers is useful when attempting to make qualitative predictions of how the sterol is distributed within cells, between bilayer leaflets, and between lateral membrane domains.

SUPPORTING MATERIAL

Supporting Materials and Methods, nine figures, and two tables are available at http://www.biophysj.org/biophysj/supplemental/S0006-3495(18)34457-6.

AUTHOR CONTRIBUTIONS

T.K.M.N., O.E., S.J., and J.P.S. planned the research. S.J., V.H., and T.K.M.N. performed the experiments. All authors analyzed the data. T.K.M.N. wrote the article, with contributions from O.E., S.J., and J.P.S.

ACKNOWLEDGMENTS

This study was supported by the Academy of Finland, the Sigrid Juselius Foundation, Medicinska Understödsföreningen Liv och Hälsa R.F., and Magnus Ehrnrooth's Foundation.

SUPPORTING CITATIONS

References (64,65) appear in the Supporting Material.

REFERENCES

1. van Meer, G., D. R. Voelker, and G. W. Feigenson. 2008. Membrane lipids: where they are and how they behave. *Nat. Rev. Mol. Cell Biol.* 9:112–124.
2. Maxfield, F. R., and G. van Meer. 2010. Cholesterol, the central lipid of mammalian cells. *Curr. Opin. Cell Biol.* 22:422–429.
3. Steck, T. L., and Y. Lange. 2018. Transverse distribution of plasma membrane bilayer cholesterol: picking sides. *Traffic.* 19:750–760.
4. Lönnfors, M., J. P. Doux, …, J. P. Slotte. 2011. Sterols have higher affinity for sphingomyelin than for phosphatidylcholine bilayers even at equal acyl-chain order. *Biophys. J.* 100:2633–2641.
5. Petruzielo, R. S., F. A. Heberle, …, G. W. Feigenson. 2013. Phase behavior and domain size in sphingomyelin-containing lipid bilayers. *Biochim. Biophys. Acta.* 1828:1302–1313.
6. Demel, R. A., J. W. Jansen, …, L. L. van Deenen. 1977. The preferential interaction of cholesterol with different classes of phospholipids. *Biochim. Biophys. Acta.* 465:1–10.
7. Engberg, O., V. Hautala, …, T. K. M. Nyholm. 2016. The affinity of cholesterol for different phospholipids affects lateral segregation in bilayers. *Biophys. J.* 111:546–556.
8. Ohvo-Rekilä, H., B. Ramstedt, …, J. P. Slotte. 2002. Cholesterol interactions with phospholipids in membranes. *Prog. Lipid Res.* 41:66–97.
9. Yasuda, T., H. Tsuchikawa, …, N. Matsumori. 2015. Deuterium NMR of raft model membranes reveals domain-specific order profiles and compositional distribution. *Biophys. J.* 108:2502–2506.
10. Nyström, J. H., M. Lönnfors, and T. K. Nyholm. 2010. Transmembrane peptides influence the affinity of sterols for phospholipid bilayers. *Biophys. J.* 99:526–533.
11. Niu, S. L., and B. J. Litman. 2002. Determination of membrane cholesterol partition coefficient using a lipid vesicle-cyclodextrin binary system: effect of phospholipid acyl chain unsaturation and headgroup composition. *Biophys. J.* 83:3408–3415.

12. van Dijck, P. W. 1979. Negatively charged phospholipids and their position in the cholesterol affinity sequence. *Biochim. Biophys. Acta.* 555:89–101.
13. Van Dijck, P. W., B. De Kruijff, …, R. A. Demel. 1976. The preference of cholesterol for phosphatidylcholine in mixed phosphatidylcholine-phosphatidylethanolamine bilayers. *Biochim. Biophys. Acta.* 455:576–587.
14. Leventis, R., and J. R. Silvius. 2001. Use of cyclodextrins to monitor transbilayer movement and differential lipid affinities of cholesterol. *Biophys. J.* 81:2257–2267.
15. Tsamaloukas, A., H. Szadkowska, …, H. Heerklotz. 2005. Interactions of cholesterol with lipid membranes and cyclodextrin characterized by calorimetry. *Biophys. J.* 89:1109–1119.
16. Bar, L. K., Y. Barenholz, and T. E. Thompson. 1987. Dependence on phospholipid composition of the fraction of cholesterol undergoing spontaneous exchange between small unilamellar vesicles. *Biochemistry.* 26:5460–5465.
17. Veatch, S. L., and S. L. Keller. 2003. Separation of liquid phases in giant vesicles of ternary mixtures of phospholipids and cholesterol. *Biophys. J.* 85:3074–3083.
18. Eggeling, C., C. Ringemann, …, S. W. Hell. 2009. Direct observation of the nanoscale dynamics of membrane lipids in a living cell. *Nature.* 457:1159–1162.
19. Levental, I., F. J. Byfield, …, P. A. Janmey. 2009. Cholesterol-dependent phase separation in cell-derived giant plasma-membrane vesicles. *Biochem. J.* 424:163–167.
20. Nyholm, T. K., D. Lindroos, …, J. P. Slotte. 2011. Construction of a DOPC/PSM/cholesterol phase diagram based on the fluorescence properties of *trans*-parinaric acid. *Langmuir.* 27:8339–8350.
21. Fischer, R. T., F. A. Stephenson, …, F. Schroeder. 1984. Delta 5,7,9(11)-Cholestatrien-3 beta-ol: a fluorescent cholesterol analogue. *Chem. Phys. Lipids.* 36:1–14.
22. Ohvo-Rekilä, H., B. Akerlund, and J. P. Slotte. 2000. Cyclodextrin-catalyzed extraction of fluorescent sterols from monolayer membranes and small unilamellar vesicles. *Chem. Phys. Lipids.* 105:167–178.
23. Kuklev, D. V., and W. L. Smith. 2004. Synthesis of four isomers of parinaric acid. *Chem. Phys. Lipids.* 131:215–222.
24. Rouser, G., S. Fkeischer, and A. Yamamoto. 1970. Two dimensional then layer chromatographic separation of polar lipids and determination of phospholipids by phosphorus analysis of spots. *Lipids.* 5:494–496.
25. Jungner, M., H. Ohvo, and J. P. Slotte. 1997. Interfacial regulation of bacterial sphingomyelinase activity. *Biochim. Biophys. Acta.* 1344:230–240.
26. Scheidt, H. A., P. Muller, …, D. Huster. 2003. The potential of fluorescent and spin-labeled steroid analogs to mimic natural cholesterol. *J. Biol. Chem.* 278:45563–45569.
27. Halling, K. K., B. Ramstedt, …, T. K. Nyholm. 2008. Cholesterol interactions with fluid-phase phospholipids: effect on the lateral organization of the bilayer. *Biophys. J.* 95:3861–3871.
28. Radhakrishnan, A., T. G. Anderson, and H. M. McConnell. 2000. Condensed complexes, rafts, and the chemical activity of cholesterol in membranes. *Proc. Natl. Acad. Sci. USA.* 97:12422–12427.
29. Huster, D., K. Arnold, and K. Gawrisch. 1998. Influence of docosahexaenoic acid and cholesterol on lateral lipid organization in phospholipid mixtures. *Biochemistry.* 37:17299–17308.
30. Garg, S., J. X. Tang, …, C. A. Naumann. 2009. Actin-induced perturbation of PS lipid-cholesterol interaction: a possible mechanism of cytoskeleton-based regulation of membrane organization. *J. Struct. Biol.* 168:11–20.
31. Ariola, F. S., Z. Li, …, A. A. Heikal. 2009. Membrane fluidity and lipid order in ternary giant unilamellar vesicles using a new bodipy-cholesterol derivative. *Biophys. J.* 96:2696–2708.
32. López, C. A., A. H. de Vries, and S. J. Marrink. 2013. Computational microscopy of cyclodextrin mediated cholesterol extraction from lipid model membranes. *Sci. Rep.* 3:2071.
33. López, C. A., A. H. de Vries, and S. J. Marrink. 2011. Molecular mechanism of cyclodextrin mediated cholesterol extraction. *PLoS Comput. Biol.* 7:e1002020.
34. Tsamaloukas, A., H. Szadkowska, and H. Heerklotz. 2006. Thermodynamic comparison of the interactions of cholesterol with unsaturated phospholipid and sphingomyelins. *Biophys. J.* 90:4479–4487.
35. Veatch, S. L., and S. L. Keller. 2005. Miscibility phase diagrams of giant vesicles containing sphingomyelin. *Phys. Rev. Lett.* 94:148101.
36. Yeagle, P. L. 1985. Cholesterol and the cell membrane. *Biochim. Biophys. Acta.* 822:267–287.
37. Bennett, W. F. D., J. E. Shea, and D. P. Tieleman. 2018. Phospholipid chain interactions with cholesterol drive domain formation in lipid membranes. *Biophys. J.* 114:2595–2605.
38. Marsh, D. 2009. Cholesterol-induced fluid membrane domains: a compendium of lipid-raft ternary phase diagrams. *Biochim. Biophys. Acta.* 1788:2114–2123.
39. Lingwood, D., and K. Simons. 2010. Lipid rafts as a membrane-organizing principle. *Science.* 327:46–50.
40. Williams, J. A., C. D. Wassall, …, S. R. Wassall. 2013. An electron paramagnetic resonance method for measuring the affinity of a spin-labeled analog of cholesterol for phospholipids. *J. Membr. Biol.* 246:689–696.
41. Pathak, P., and E. London. 2015. The effect of membrane lipid composition on the formation of lipid ultrananodomains. *Biophys. J.* 109:1630–1638.
42. Baumgart, T., G. Hunt, …, G. W. Feigenson. 2007. Fluorescence probe partitioning between Lo/Ld phases in lipid membranes. *Biochim. Biophys. Acta.* 1768:2182–2194.
43. Scheidt, H. A., T. Meyer, …, D. Huster. 2013. Cholesterol's aliphatic side chain modulates membrane properties. *Angew. Chem. Int.Engl.* 52:12848–12851.
44. Halling, K. K., and J. P. Slotte. 2004. Membrane properties of plant sterols in phospholipid bilayers as determined by differential scanning calorimetry, resonance energy transfer and detergent-induced solubilization. *Biochim. Biophys. Acta.* 1664:161–171.
45. Leppimäki, P., J. Mattinen, and J. P. Slotte. 2000. Sterol-induced upregulation of phosphatidylcholine synthesis in cultured fibroblasts is affected by the double-bond position in the sterol tetracyclic ring structure. *Eur. J. Biochem.* 267:6385–6394.
46. Konyakhina, T. M., and G. W. Feigenson. 2016. Phase diagram of a polyunsaturated lipid mixture: brain sphingomyelin/1-stearoyl-2-docosahexaenoyl-sn-glycero-3-phosphocholine/cholesterol. *Biochim. Biophys. Acta.* 1858:153–161.
47. Konyakhina, T. M., J. Wu, …, G. W. Feigenson. 2013. Phase diagram of a 4-component lipid mixture: DSPC/DOPC/POPC/chol. *Biochim. Biophys. Acta.* 1828:2204–2214.
48. Cornell, C. E., N. L. C. McCarthy, …, S. L. Keller. 2017. n-Alcohol length governs shift in L_o-L_d mixing temperatures in synthetic and cell-derived membranes. *Biophys. J.* 113:1200–1211.
49. Bleecker, J. V., P. A. Cox, and S. L. Keller. 2016. Mixing temperatures of bilayers not simply related to thickness differences between Lo and Ld phases. *Biophys. J.* 110:2305–2308.
50. Björkqvist, Y. J., T. K. Nyholm, …, B. Ramstedt. 2005. Domain formation and stability in complex lipid bilayers as reported by cholestatrienol. *Biophys. J.* 88:4054–4063.
51. Cui, J., S. Lethu, …, M. Murata. 2015. Phosphatidylcholine bearing 6,6-dideuterated oleic acid: a useful solid-state (2)H NMR probe for investigating membrane properties. *Bioorg. Med. Chem. Lett.* 25:203–206.
52. Veatch, S. L., I. V. Polozov, …, S. L. Keller. 2004. Liquid domains in vesicles investigated by NMR and fluorescence microscopy. *Biophys. J.* 86:2910–2922.
53. Ionova, I. V., V. A. Livshits, and D. Marsh. 2012. Phase diagram of ternary cholesterol/palmitoylsphingomyelin/palmitoyloleoyl-phosphatidylcholine mixtures: spin-label EPR study of lipid-raft formation. *Biophys. J.* 102:1856–1865.

54. Zhao, J., J. Wu, …, G. W. Feigenson. 2007. Phase studies of model biomembranes: complex behavior of DSPC/DOPC/cholesterol. *Biochim. Biophys. Acta.* 1768:2764–2776.

55. Wang, C., M. R. Krause, and S. L. Regen. 2015. Push and pull forces in lipid raft formation: the push can be as important as the pull. *J. Am. Chem. Soc.* 137:664–666.

56. Huang, J., J. T. Buboltz, and G. W. Feigenson. 1999. Maximum solubility of cholesterol in phosphatidylcholine and phosphatidylethanolamine bilayers. *Biochim. Biophys. Acta.* 1417:89–100.

57. Ingólfsson, H. I., T. S. Carpenter, …, F. C. Lightstone. 2017. Computational lipidomics of the neuronal plasma membrane. *Biophys. J.* 113:2271–2280.

58. Ingólfsson, H. I., M. N. Melo, …, S. J. Marrink. 2014. Lipid organization of the plasma membrane. *J. Am. Chem. Soc.* 136:14554–14559.

59. Mondal, M., B. Mesmin, …, F. R. Maxfield. 2009. Sterols are mainly in the cytoplasmic leaflet of the plasma membrane and the endocytic recycling compartment in CHO cells. *Mol. Biol. Cell.* 20:581–588.

60. Bakht, O., P. Pathak, and E. London. 2007. Effect of the structure of lipids favoring disordered domain formation on the stability of cholesterol-containing ordered domains (lipid rafts): identification of multiple raft-stabilization mechanisms. *Biophys. J.* 93:4307–4318.

61. Engberg, O., T. Yasuda, …, J. P. Slotte. 2016. Lipid interactions and organization in complex bilayer membranes. *Biophys. J.* 110:1563–1573.

62. Wang, T. Y., and J. R. Silvius. 2001. Cholesterol does not induce segregation of liquid-ordered domains in bilayers modeling the inner leaflet of the plasma membrane. *Biophys. J.* 81:2762–2773.

63. Wassall, S. R., and W. Stillwell. 2009. Polyunsaturated fatty acid-cholesterol interactions: domain formation in membranes. *Biochim. Biophys. Acta.* 1788:24–32.

64. Nyholm, T. K., P. M. Grandell, …, J. P. Slotte. 2010. Sterol affinity for bilayer membranes is affected by their ceramide content and the ceramide chain length. *Biochim. Biophys. Acta.* 1798:1008–1013.

65. Yasuda, T., M. A. Al Sazzad, …, J. P. Slotte. 2016. The influence of hydrogen bonding on sphingomyelin/colipid interactions in bilayer membranes. *Biophys. J.* 110:431–440.

Biophysical Journal, Volume *116*

Supplemental Information

The Affinity of Sterols for Different Phospholipid Classes and Its Impact on Lateral Segregation

Thomas K.M. Nyholm, Shishir Jaikishan, Oskar Engberg, Victor Hautala, and J. Peter Slotte

Supporting material

The affinity of sterols for different phospholipid classes and its impact on lateral segregation

T.K.M. Nyholm*, S. Jaikishan, O. Engberg, V. Hautala and J. P. Slotte

Methods

Equilibrium distribution of CTL between mβCD and large unilamellar vesicles

CTL partitioning between large unilamellar vesicles (LUVs) and mβCD was measured as described previously (1, 2). In brief, multilamellar vesicles of different PLs with 2 mol% CTL were prepared in buffer. LUVs were prepared by extrusion using membranes with 100-nm pores (Whatman International, Maidstone, UK). The LUVs (final concentration 0.4 mM) were mixed with cyclodextrin (0–1 mM), and the samples were incubated until the equilibrium distribution of CTL between LUVs and cyclodextrin was reached. The steady-state anisotropy of CTL was measured in samples with different mβCD concentrations, and the molar concentration of CTL, C_{CTL}^{LUV}, in the LUVs in each sample was calculated from the measured anisotropies according to

$$C_{CTL}^{LUV} = C_{CTL}\frac{(r_i - r_{CD})}{(r_{LUV} - r_{CD})} \quad [1]$$

where C_{CTL} is the total concentration of CTL in the samples, r_{LUV} is the anisotropy of CTL in the specific PL bilayer, r_i is the CTL anisotropy in the sample, and r_{CD} is the anisotropy of CTL in the CTL–mβCD complex. K_X was calculated by plotting the calculated molar concentrations of CTL in the PL bilayers against the mβCD concentration and fitting the obtained curves with the following equation:

$$C_{CTL}^{LUV} = \frac{C_L - C_{CTL} + (C_{CD})^n/K_X}{2} \times \left(\sqrt{1 + 4\frac{C_L C_{CTL}}{[C_L - C_{CTL} + (C_{CD})^n/K_X]^2}} - 1\right) \quad [2]$$

Here, C_L is the PL concentration, C_{CD} is the cyclodextrin concentration, and C_{CTL}^{LUV} is the cholesterol concentration in lipid bilayers. The PL concentration was determined after anisotropy measurements in all samples so that the correct concentration was used in the calculations. For this, the samples were freeze dried and re-dissolved in methanol, and the PL concentration was determined according to Rouser et al (3). The relative partitioning coefficient K_R was calculated by dividing the K_X obtained with different PL samples with the K_X obtained from samples with only POPC.

Equilibrium distribution of cholesterol between donor and acceptor vesicles

The equilibrium partitioning of cholesterol between large unilamellar donor vesicles (donor LUVs) and large unilamellar acceptor vesicles (acceptor LUVs) was determined using an anisotropy-based assay. Donor LUVs were composed of POPC, 25 mol% cholesterol and

DPH-PC (1 mol%). In studies of unsaturated PL-cholesterol interactions, the acceptor LUVs were composed of pure POPC, OSM, POPE, POPS or POPG. When the interactions between cholesterol and saturated PLs was studied the acceptor LUVs were composed of 80 mol% POPC and 20 mol% DPPC, PSM, DPPE, DPPS, or DPPG. LUVs were prepared as follows. First, the lipids were mixed in organic solvent, and then the solvent was evaporated under a constant stream of nitrogen. The dry lipid film was hydrated in buffer at 60 ºC, after which it was vigorously vortexed and bath sonicated at 60 ºC for 5 minutes. To prepare the LUVs, the vesicles were passed through membranes with a pore size of 100 nm 11 times using an Avanti Mini-Extruder (Avanti Polar Lipids, Alabaster, AL). The PL concentrations were determined after extrusion according to a published procedure (3).

For the experiment, 50 μM donor and 50 μM acceptor LUVs (PL concentration) were mixed together in a glass tube and incubated overnight at 37 ºC, after which the steady-state anisotropy of DPH-PC in the donor LUVs was measured. The amount of cholesterol in the donor LUVs was determined using a standard curve, which was determined for POPC with 0 to 30 mol% cholesterol and 1 mol% DPH-PC at the appropriate temperature. When the total amount of cholesterol was known (determined from the standard curve in samples consisting of only donor LUVs), the cholesterol content in the acceptor LUVs could be calculated, and K_R could also be calculated by dividing the amount of cholesterol in the acceptor LUVs with that in the donor LUVs.

Equilibrium distribution of TF-cholesterol between donor and acceptor vesicles

The distribution of TF-cholesterol between large unilamellar donor vesicles (donor LUVs) and large unilamellar acceptor vesicles (acceptor LUVs) was studied using a Förster resonance energy transfer (FRET) approach, in which the FRET donor was DPH-PC and the FRET acceptor was TF-cholesterol. Donor LUVs were prepared from 100 nmol PL POPC and 0.5 mol% DPH-PC and 0.5 mol% TF-cholesterol. Acceptor vesicles were prepared from 100 nmol PLs. Lipids and fluorophores were mixed in organic solvent, and then the solvent was evaporated under a constant stream of N_2 at 40 ºC. The dry films were re-dissolved in chloroform, and subsequently the solvent was again evaporated. The dry lipid film was hydrated at 60 ºC and vortexed vigorously. The resulting multilamellar vesicles were then filtered 11 times through a polycarbonate filter with a pore size of 100 nm (Whatman International, Maidstone, UK) above 60 ºC. The quality of the formed LUVs was verified with a Malvern Zetasizer Nano-S (Malvern Instruments, Worcestershire, UK).

Donor and acceptor LUVs were mixed in water (total lipid concentration 80 μM) and 0.5 mM mβCD. The donor/acceptor LUV ratio was 1 if not otherwise mentioned. All samples were then incubated at 37 ºC overnight to ensure equilibrium partitioning. Next, the fluorescence lifetime of DPH-PC was measured at the equilibration temperature using a PicoQuant Fluotime 200 spectrometer (PicoQuant, Berlin, Germany) mounted with a 378 nm PDL 800-D pulsed diode laser and a PicoHarp event timer. In addition, the lifetime of DPH-PC in the donor LUVs without cyclodextrin and acceptor LUVs (τ_{INI}) and the lifetime of DPH-PC in donor LUVs without TopFlour-cholesterol (τ_0) were measured at the indicated temperature. The average lifetimes of all samples were calculated using Fluofit software (PicoQuant).

From the time-resolved data, the FRET efficiency (E) was calculated for all samples according to

$$E = 1 - \frac{\tau_i}{\tau_0} \quad [3]$$

As the FRET efficiency has a linear dependence on the concentration of TopFlour-cholesterol in the donor LUVs, the fraction of TopFlour-cholesterol in the donor LUVs (X_D) could be calculated from the FRET efficiency using the following equation (assuming that E is 0 upon total removal of TopFlour-cholesterol from the donor LUVs):

$$X_D = \frac{E_{INI} - E_i}{E_{INI}} \quad [4]$$

where E_{INI} is the FRET efficiency without transfer (with donor LUVs only) and E_i is the FRET efficiency in the particular mixture of donor and acceptor LUVs. When the molar fractions of TopFlour-cholesterol in donor and acceptor LUVs are known, the partitioning coefficient (K) can be calculated according to

$$K = \frac{X_A C_A}{X_D C_D} \quad [5]$$

where X_A and X_D are the molar fraction sterols in the acceptor and donor LUVs and C_A and C_D are the concentrations of acceptor and donor LUVs. The K values are normalized to the K obtained for POPC–POPC partitioning (which was always close to equality), which gives the K_R.

Results

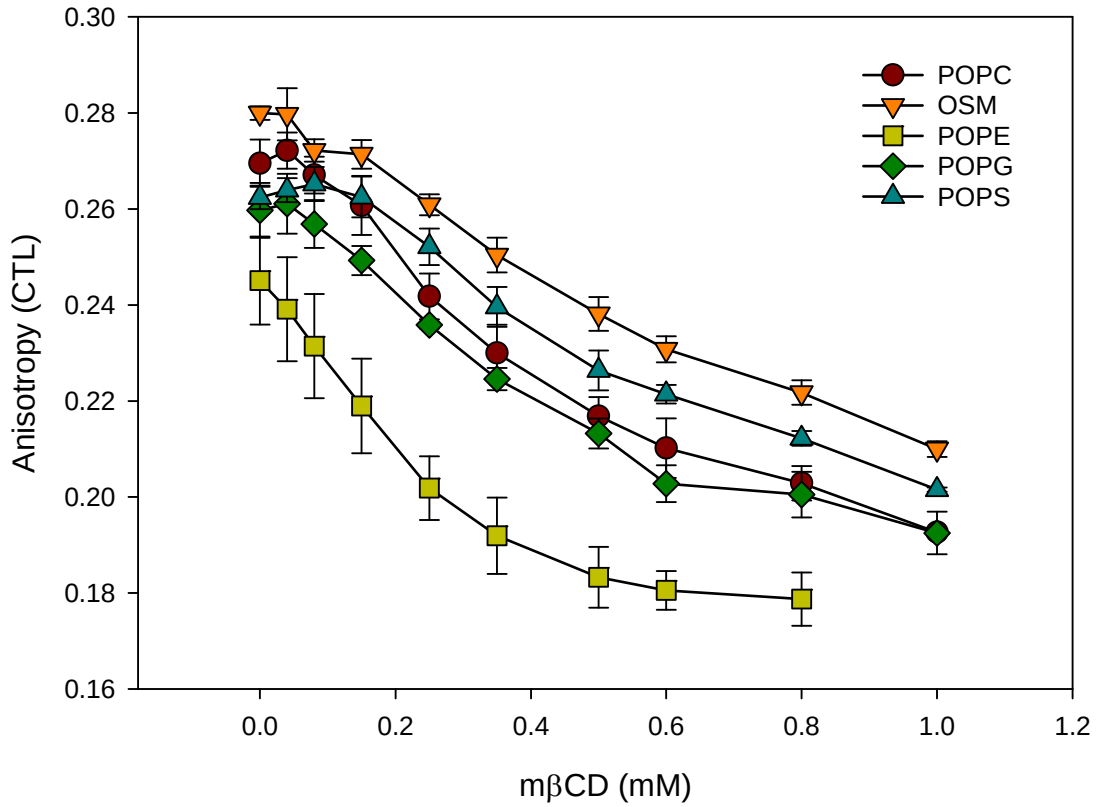

Figure S1. Equilibrium partitioning of cholestratrienol between LUVs and methyl-β-cyclodextrin. Representative data from experiments where the anisotropy of CTL was measured in samples containing different PL vesicles and 0–1.0 mM mβCD. All experiments were performed at 37 ºC.

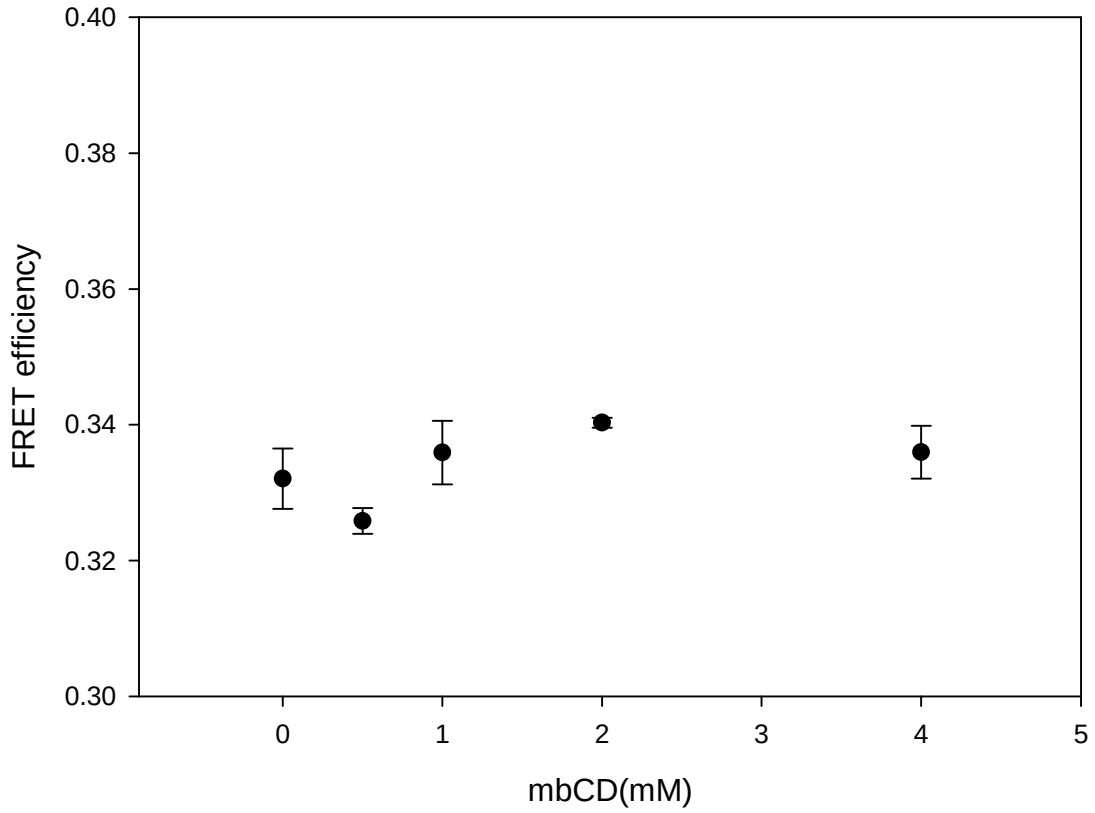

Figure S2. TopFluor-cholesterol was not removed from phospholipid bilayers by mβCD. When measuring FRET between DPH-PC and TopFluor-cholesterol in POPC bilayers in the presence of increasing amounts of mβCD no impact on the FRET efficiency was observed. This suggests that TopFluor-cholesterol was not taken up by mβCD. The experiments were made at 37 ºC, and the values are averages $\pm$ SD with n = 3.

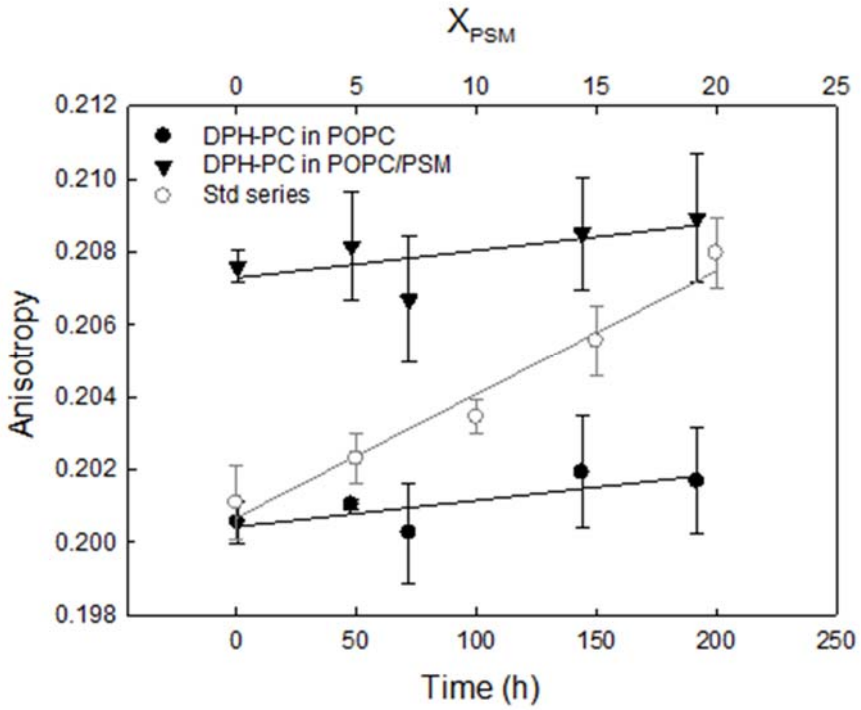

Figure S3. DPH-PC was not transferred between donor and acceptor LUVs. The anisotropy of DPH-PC was measured at 37 ºC in POPC LUVs mixed with POPC/PSM (80:20) LUVs without fluorophores and vice versa. During 200 h of measurements, the DPH-PC anisotropy remained unchanged, indicating that no exchange of probe between the vesicles occurred. The standard curve shows the DPH-PC anisotropy at the same temperature in POPC bilayers as a function of PSM content. Values are average $\pm$ SD with n = 3.

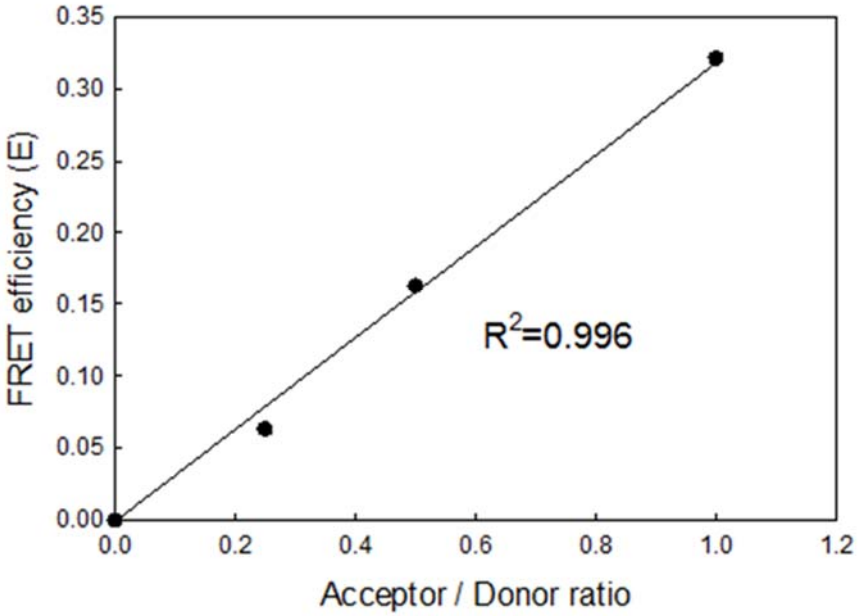

Figure S4. The FRET efficiency had a linear dependency on the acceptor/donor ratio in the concentration range used in the experiments. The FRET efficiency between DPH-PC and TopFluor-cholesterol was determined in POPC LUVs at 37 ºC at different acceptor/donor ratios with a constant DPH-PC concentration. The data in this figure is representative.

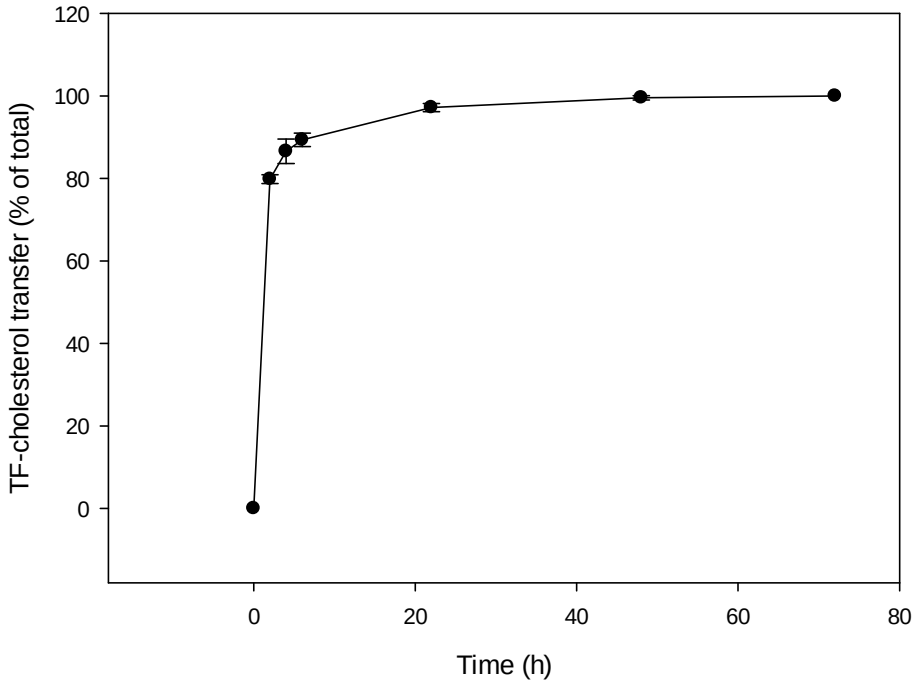

Figure S5. The time-dependence of TF-cholesterol transfer between donor POPC and POPC/PSM (80:20) acceptor LUVs. Donor and acceptor LUVs were mixed 1:1 and incubated at 37 ºC. The FRET efficiency between DPH-PC and TF-cholesterol was measured as a function of time, and transfer percentage was calculated from this data.

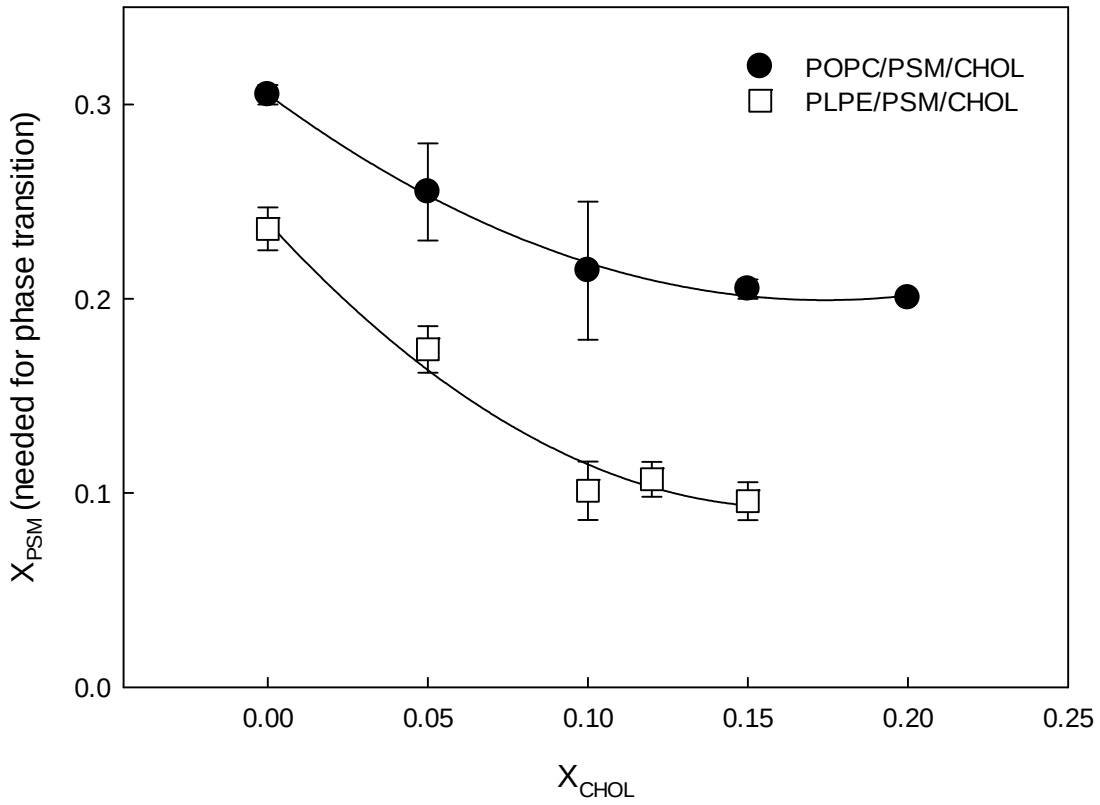

Figure S6. The effect of cholesterol on lateral segregation in PLPE/PSM/Cholesterol bilayers. The formation of gel or l_o domains was determined from tPA lifetimes measured at 23°C. For comparison, the data for the POPC/PSM/cholesterol systems is included. The values are averages $\pm$ SD with n = 3.

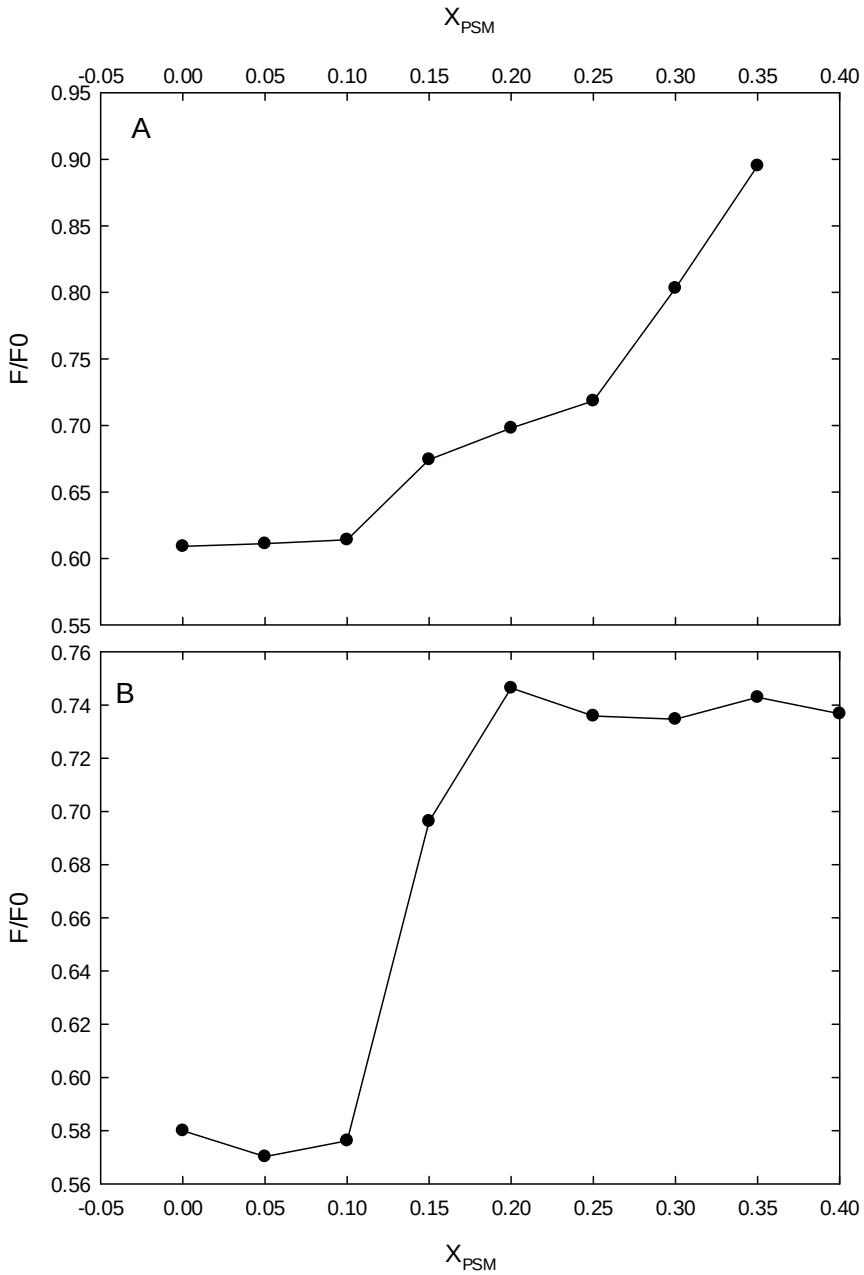

Figure S7. The formation of l_o domains in PLPE/PSM/CHOL bilayers as determined by FRET at 23 ^oC. Using the FRET pair DPH (0.1 mol%) and rhodamine-DOPE (0.5 mol%) the formation of nanodomains can be determined (4). In the PLPE/PSM/CHOL bilayers with both 15 (panel A) and 20 mol% cholesterol (panel B), F/F_0 was more or less unchanged up to 10 mol% PSM, after which it clearly increased. This decrease in FRET efficiency was likely due to the formation of l_o domains, into which only DPH partitioned, which in turn led to a partial separation of DPH and rhodamine-PE in the bilayers. We therefore interpret the data to show that the l_o domains started to form at this ($X_{PSM} = 0.10$) PSM content. The data is representative data from two separate experiments.

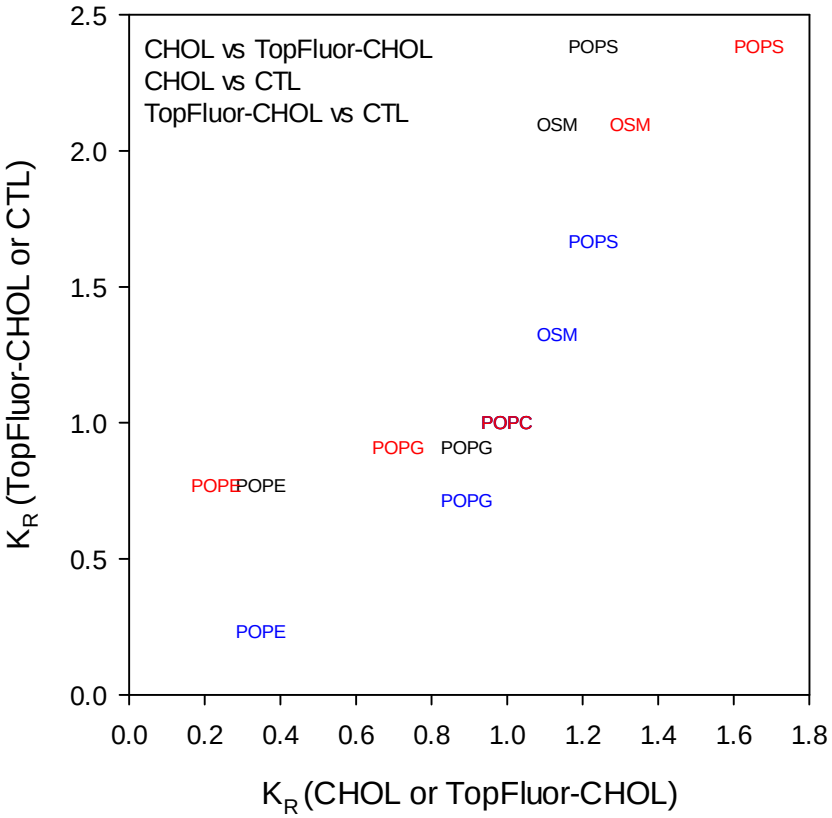

Figure **S8.** Comparison of the partitioning behavior of TopFluor-cholesterol, CTL and cholesterol. To compare the data obtained with the three sterols the K_R determined with one sterol were plotted against another. The K_R values for the sterol first mentioned is shown on the x-axis and values for the second sterol is shown on the y-axis. The values are average values.

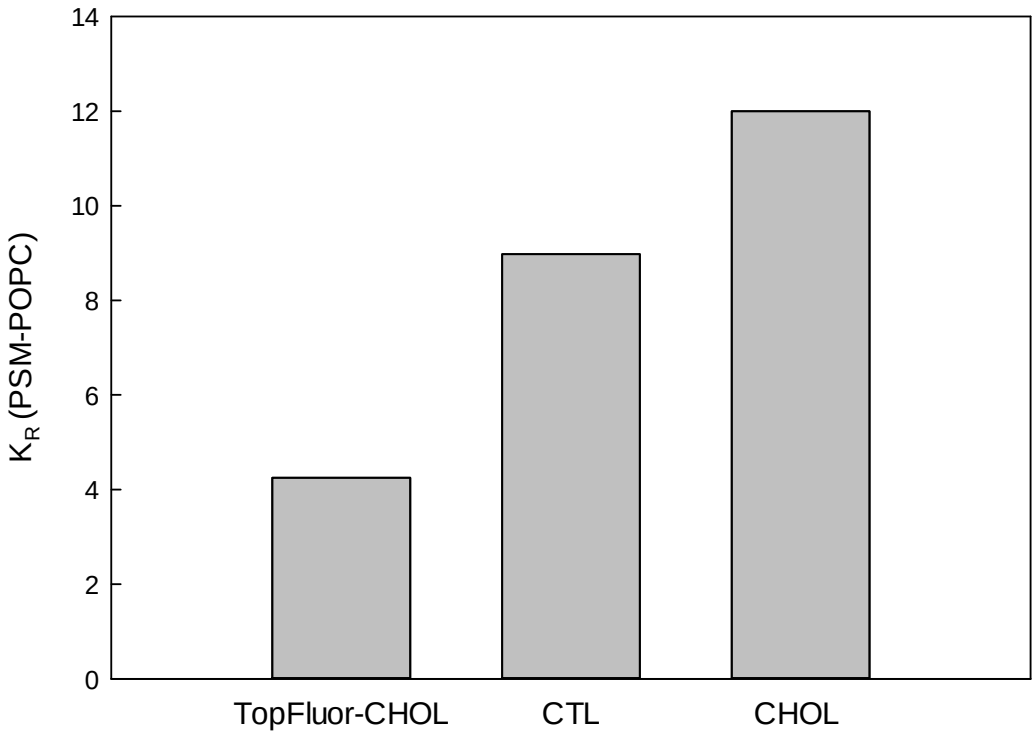

Figure S9. The relative partitioning coefficients determined for the partitioning of different sterols between POPC and PSM LUVs. TopFluor-cholesterol partitioning results obtained at 50 ºC are from (5), the CTL data is from the this work (at 37 ºC) and the PSM data (50 ºC) from (5, 6). The K_R for cholesterol at 50 ºC was obtained from (7). For CTL we were not able to determine the K_R at 50 ºC due to the low fluorescence at this temperature. The values were calculated from two average values.

Table S1. Gibbs free energies for transfer of sterols from POPC to other phospholipids.[a]

Phospholipid	**ΔG (kcal/mol)**		
	CTL	**TF-cholesterol**	**Cholesterol**
POPE	1.08	3.80	2.72
POPG	0.25	0.88	0.29
OSM	-1.91	-0.72	-0.32
POPS	-2.18	-1.32	-0.53
POPC/DPPE	0.32		0.17
POPC/DPPG	-0.41		-0.03
POPC/DPPS	-0.80		-0.06
POPC/DPPC	-1.35		-0.14
POPC/PSM	-1.95		-0.35

[a] All Gibbs free energies where calculated from the K_R values obtains experimentally at 37 ^{o}C with the different sterols. Gibbs free energies for the transfer of sterol from the POPC to bilayers composed of other phospholipids were calculated using the following equation: $\Delta G = -RT \ln K$.

Table S2. Estimated distribution of sterols between the inner and outer leaflets [a]

Average membranes [b]	Cholestatrienol	Cholesterol	TopFluor-cholesterol
Average K (inner)	2.26	2.40	1.28
Average K (outer)	3.48	4.43	1.96
K (outer/inner)	1.54	1.84	1.53
ΔG (kcal/mol)	-1.11	-1.57	-1.09
Fraction of sterol (inner)	0.39	0.35	0.40
Fraction of sterol (outer)	0.61	0.65	0.60

Brain membranes [b]	Cholestatrienol	Cholesterol	TopFluor-cholesterol
Average K (inner)	1.51	0.95	1.29
Average K (outer)	2.51	1.46	3.06
K (outer/inner)	1.67	1.54	1.54
ΔG (kcal/mol)	-1.32	-2.23	-1.54
Fraction of sterol (inner)	0.38	0.30	0.39
Fraction of sterol (outer)	0.62	0.70	0.61

[a] The distribution of cholestatrienol, cholesterol and TopFluor-cholesterol between the inner and outer leaflet of the plasma membranes was calculated using the partitioning coefficients determined for the different sterols between different phospholipid bilayers. First, the Average K for the inner and outer leaflets was calculated by combining the partitioning coefficients of all phospholipid types in the leaflet and normalizing them according to the fraction of each lipid class present in the leaflet. Then K (outer/inner) was calculated by dividing Average K (outer) with Average K (inner). This parameter was then used to calculate the fraction of the different sterols in the two leaflets. Gibbs free energies for the transfer of sterol from the inner to the outer leaflet were calculated from the K (outer/inner) using the following equation: $\Delta G = -RT \ln K$.

[b] The lipid composition in the bilayers that the calculations were based on was based on the composition used in (8).

Supporting References

1. Nyholm, T. K., P. M. Grandell, B. Westerlund, and J. P. Slotte. 2010. Sterol affinity for bilayer membranes is affected by their ceramide content and the ceramide chain length. Biochim Biophys Acta 1798:1008-1013.

2. Nyström, J. H., M. Lönnfors, and T. K. M. Nyholm. 2010. Transmembrane Peptides Influence the Affinity of Sterols for Phospholipid Bilayers. Biophys J 99(2) In press.
3. Rouser, G., S. Fkeischer, and A. Yamamoto. 1970. Two dimensional then layer chromatographic separation of polar lipids and determination of phospholipids by phosphorus analysis of spots. Lipids 5:494-496.
4. Pathak, P., and E. London. 2015. The Effect of Membrane Lipid Composition on the Formation of Lipid Ultrananodomains. Biophys J 109:1630-1638.
5. Engberg, O., V. Hautala, T. Yasuda, H. Dehio, M. Murata, J. P. Slotte, and T. K. Nyholm. 2016. The Affinity of Cholesterol for Different Phospholipids Affects Lateral Segregation in Bilayers. Biophys J 111:546-556.
6. Yasuda, T., M. A. Al Sazzad, N. Z. Jantti, O. T. Pentikainen, and J. P. Slotte. 2016. The Influence of Hydrogen Bonding on Sphingomyelin/Colipid Interactions in Bilayer Membranes. Biophys J 110:431-440.
7. Tsamaloukas, A., H. Szadkowska, and H. Heerklotz. 2006. Thermodynamic comparison of the interactions of cholesterol with unsaturated phospholipid and sphingomyelins. Biophys J 90:4479-4487.
8. Ingolfsson, H. I., T. S. Carpenter, H. Bhatia, P. T. Bremer, S. J. Marrink, and F. C. Lightstone. 2017. Computational Lipidomics of the Neuronal Plasma Membrane. Biophys J 113:2271-2280.